JOURNAL OF EXPERIMENTAL AND THEORETICAL PHYSICS, 2024, Vol. 166, No. 1(7), pp. 8–17

MICROWAVE INDUCED RESISTANCE OSCILLATIONS IN TWO DIMENSIONAL ELECTRON SYSTEMS

© 2024 A. V. Shchepetilnikov*, I. V. Kukushkin**

Osipyan Institute of Solid State Physics
RAS 142432, Chernogolovka, Moscow region, Russia

** e-mail: shchepetilnikov@issp.ac.ru*
*** e-mail: kukush@issp.ac.ru*

Received February 21, 2024
Revised March 24, 2024
Accepted March 24, 2024

Abstract. The most important features of microwave induced resistance oscillations in two-dimensional electron systems are considered. The possibility of observing this phenomenon in various material systems using different experimental techniques, including contactless ones, is discussed. Special attention is paid to the influence of electron-electron interaction on the oscillation period, as well as the necessity of depositing metallic layers near the two-dimensional electron system.

Article for the special issue of JETP dedicated to the 130th anniversary of P. L. Kapitsa

DOI: 10.31857/S004445102407e022

1. INTRODUCTION

At low temperatures the high quality two-dimensional electron system subject to the high-frequency radiation exhibit pronounced oscillations of the longitudinal magnetoresistance [1, 2]. The radiation induced correction ΔR_{xx} is periodic in inverse magnetic field, and the period of such oscillations is determined by the commensurability between the radiation frequency and cyclotron energy. The magnitude of the correction ΔR_{xx} is well described by the phenomenological expression

$$\Delta R_{xx} = -\epsilon A \sin(2\pi\epsilon + \varphi)\exp(-\alpha\epsilon). \qquad (1)$$

Here the parameter $\epsilon = \omega / \omega_c$ is the ratio of electromagnetic radiation frequency to cyclotron energy, A — the amplitude of the effect, α determines the effect's decay with increasing oscillation number as external magnetic field decreases, and φ is the oscillation phase. Strictly speaking, in the denominator of expression for $\omega_c = eB / m^*$ stands not the cyclotron mass but some effective mass renormalized due to Fermi-liquid effects. This phenomenon will be discussed further in our review. In works [3, 4], it was shown that typically φ equals zero, but under certain conditions φ can deviate from this value, especially for the first oscillation [5–8]. The amplitude of the effect A depends on the incident radiation power, it is linear in the low-power region and follows a square root dependence in the high-power regime [9].

The phenomenon of electromagnetic radiation-induced oscillations was first discovered over 20 years ago [1] during the study of transport response in two-dimensional electron systems confined in various quantum wells and GaAs/AlGaAs heterostructures. The material parameters of the samples naturally determined the radiation frequency range – from several gigahertz to several tens of gigahertz, which effectively led to the formation of a stable term denoting the phenomenon under consideration – microwave induced resistance oscillations (MIRO) of magnetoresistance.

The discovery of this effect was followed by extensive research, which formed an entire direction in condensed matter physics. Thus, the dependencies of oscillation phase on their number were measured [5], the attenuation of the effect amplitude was studied at different temperatures [10–12] and in tilted magnetic fields [4, 13]. A whole family of effects

related to the phenomenon under consideration was discovered. Under certain conditions, the oscillation amplitude increased so much that the total system resistance became negative, leading to instability in the electronic system and its division into current and charge domains [14–16]. The total resistance of the two-dimensional system turned out to be zero over a fairly wide range of magnetic fields, effectively forming a zero-resistance state [17, 18]. Similar oscillations were also observed in the capacitive characteristics of the two-dimensional electron system [19, 20], as well as in the photovoltage and photocurrent arising at contacts to the two-dimensional electron system [21–24]. It was demonstrated that similar magnetoresistance oscillations could also be induced by Hall voltage [25–28] and electron-phonon interactions [29, 30].

A number of well-developed theories [31–39] have been proposed to form a complete physical picture of this phenomenon. Most of these theories are based on the absorption of microwave radiation by conduction electrons in the Drude model, the magnitude of which depends on the degree of circular polarization of light as $1/[(\omega \pm \omega_c)^2 + 1/\tau^2]$. Here τ is the characteristic scattering time. The "plus" and "minus" signs correspond to different circular polarization of light. This expression determines, for example, the sensitivity of cyclotron resonance to radiation polarization. However, unlike cyclotron resonance, the influence of radiation polarization on the amplitude of resistance oscillations in a two-dimensional channel is still a subject to discussion, and experiments by different groups yield contradictory results [40–42]. All this led to the emergence of alternative models, within which resistance oscillations arise from interaction with microwave radiation not of all electrons, but only of some portion localized either near the sample edge [43, 44] or in regions near ohmic contacts or metallic layer deposited on the surface of the sample [45]. In such regions, the incident radiation effectively loses its polarization state, and the effect's sensitivity to the degree of circular polarization of radiation should disappear. Relatively recently, the absorption of electromagnetic radiation by electrons in some vicinity of impurities and inhomogeneities of the two-dimensional system was considered [46], which also resulted in the loss of sensitivity of oscillation amplitude to the degree of circular polarization of radiation.

Thus, despite all efforts, several crucial features of the observed effect still do not fit well into this picture. Besides the insensitivity of oscillations to the degree of circular polarization of incident radiation, we can also note the decrease in effective mass calculated from the oscillation period compared to the cyclotron mass [47–50]. These contradictions maintain the continuing relevance of studying microwave radiation-induced resistance oscillations. Another important direction of modern research is expanding the set of material systems in which these oscillations are observed, which in perspective will allow a much fuller understanding of the phenomenon under consideration. The mentioned aspects of MIRO will be discussed in more detail further in our review.

2. EXPERIMENTAL METHODOLOGY

Generally, standard transport techniques are suitable for experimental study of magnetoresistance oscillations induced by electromagnetic radiation. Typically, standard Hall bars with drain, source, and several potentiometric contacts are formed on the samples. Note that other contact geometries were also tested – Corbino disk [51] and van der Pauw geometry [16, 24]. The sample is placed inside a cryostat equipped with a superconducting magnet, so that the two-dimensional electron system is cooled to temperatures of 1 K and below. Above the sample, there is a waveguide or a coaxial cable terminated with an antenna, through which electromagnetic radiation is delivered to the sample. Sometimes, to concentrate the electric field near the two-dimensional electron system a coplanar waveguide is formed on the sample surface. The excitation radiation is then transmitted through this waveguide [52]. Experimental studies of the polarization dependencies of MIRO are performed using quasi-optical setups with special cryostats equipped with windows transparent in the correspondent frequency range. With such an excitation scheme, the polarization state of the radiation can be set with good and may be controlled by analyzing the cyclotron resonance in the sample.

For precise measurement of the longitudinal resistance of the two-dimensional channel, a lock-in amplifier is used, with the amplitude of the alternating current selected in such a way that the electronic system is not overheated. The correction ΔR_{xx} is obtained by comparing the magnetoresistance of the two-dimensional channel under radiation

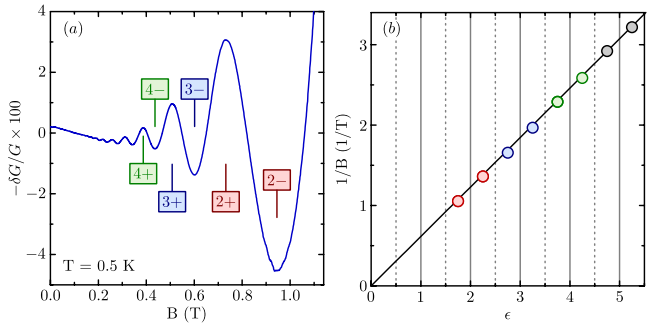

Fig. 1. (In color online) *a* — Oscillations of the magnetoconductivity *G* of two-dimensional electron system confined in a heterojunction ZnO/MgZnO. The radiation frequency was 140 ГГц. The experimental temperature $T = 1.5$ K. *b* — Dependence of the inverse magnetic field corresponding to the oscillation extrema on their number. The sample, radiation frequency, and temperature are the same as for panel *a*

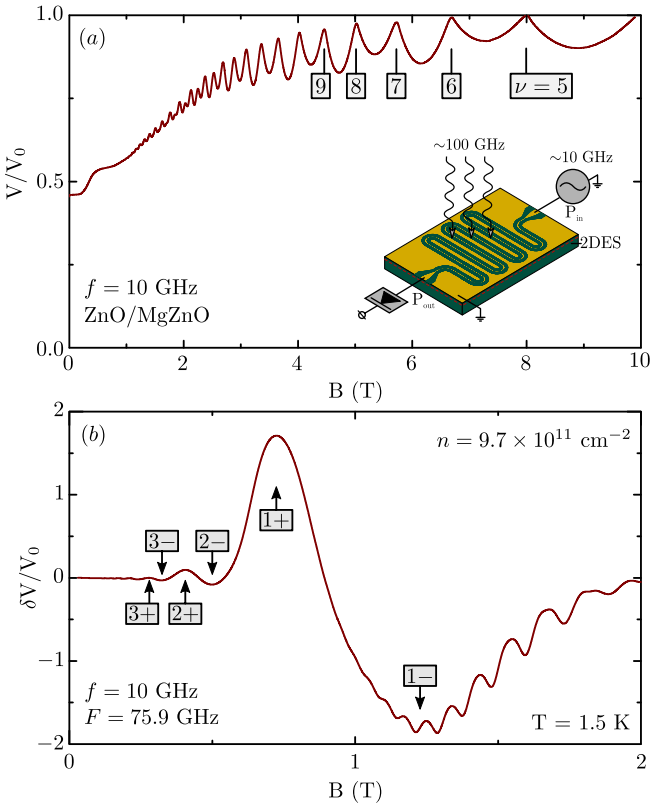

Fig. 2. (In color online) *a* — Dependence of the detector signal at the output of the coplanar waveguide deposited on the sample surface on the magnetic field. The frequency of radiation passed through the sample is 10 GHz. The sample was a heterojunction ZnO/MgZnO with two-dimensional electron density $9.7 \cdot 10^{11}$ cm^{-2}. Sample temperature was 1.5 K. The position of the first several filling factors is marked. The inset shows the experimental setup. *b* — Typical microwave induced resistance oscillations observed in such a scheme. The excitation radiation frequency is 75.9 GHz, and the probe frequency is 10 GHz

exposure and without it. The electromagnetic radiation frequency remains fixed while the magnetic field is swept. To improve the signal-to-noise ratio, a standard double lock-in detection technique can be used. In this case, the radiation incident on the sample is amplitude-modulated. The first lock-in amplifier, tuned to the alternating current frequency, effectively measures the resistance of the two-dimensional channel. The second amplifier, tuned to the frequency of the radiation modulation, takes the signal from the output of the first one and measures the signal proportional to the variation ΔR_{xx}. This experimental approach allows to observe radiation-induced resistance oscillations even in less perfect two-dimensional systems where the effect is relatively weak.

An example of a correction δG to the magnetoconductivity of the sample, measured in a heterojunction ZnO/MgZnO, containing a two-dimensional electron system, is shown in Fig. 1 *a*. The sample temperature was 1.5 K. The sample was made in the geometry of a Corbino disk. The radiation frequency was 140 GHz. It is clearly visible that this correction is periodic in inverse magnetic field and decays in the region of low fields – high oscillation order numbers. The numbers of the first few oscillations are marked in the figure.

According to formula (1), the maxima and minima of oscillations correspond to values $\epsilon = k \pm 1/4$, where $k = 1,2,3\ldots$ To verify this fact, one can analyze the dependence of the inverse magnetic field corresponding to the extrema of oscillations on ε, where the minimum with number k will correspond to value $k - 1/4$, and the maximum with the same number — $k + 1/4$. In Fig. 1 *b* we show such dependence calculated from the data presented in the panel (*a*) of the same figure. It is clearly visible that in such coordinates, the dependence of the oscillation extrema position on the order number is linear, and the line passes through the origin, which clearly indicates zero phase of the oscillations. Note that, typically, the phase φ becomes non-zero only for the first oscillation.

The oscillation amplitude decays exponentially with increasing oscillation number (or, equivalently, with decreasing magnetic field). Such behavior is very well noticeable in Fig. 1 *a*. It is believed that such damping is caused by the broadening of Landau levels due to system imperfections. In this case the value α in formula (1) is determined

by the inverse quantum lifetime τ_q. It should be emphasized that this characteristic time differs from the transport scattering time. For example, in typical heterostructures ZnO/MgZnO and GaAs/AlGaAs the value τ_q is approximately 5 and 15 ps respectively and differs only by a factor of three, while transport mobilities in GaAs structures are higher by almost two orders of magnitude [24]. On the other hand, the time τ_q also does not coincide with the time τ, which determines the damping of Shubnikov–de Haas oscillation amplitude in weak magnetic fields and at elevated temperatures. This is because, unlike MIRO, the Shubnikov–de Haas oscillation period is linear with respect to two-dimensional electron density, meaning their amplitude damping is largely determined by concentration uniformity in the two-dimensional system.

Along with standard transport methods, contactless techniques for detecting microwave radiation-induced resistance oscillations have been developed. Transport characteristics may be effectively measured without forming ohmic contacts to the two-dimensional layer. In this case the resistance or conductivity of the electronic system are characterized at high frequency (from several megahertz to tens of gigahertz). In part, the application of such approaches was driven by attempts to understand one of the fundamental questions – what influence do the regions of ohmic contacts and areas near metallic layers deposited on the sample surface have on the physics of MIRO.

The interaction of a two-dimensional electron system with electromagnetic radiation determines of the channel, and therefore, analysis of transmission or absorption of radiation in the system allows contactless measurement of this value [53, 54]. In works [55, 56] the possibility of observing resistance oscillations was demonstrated by analyzing the transmission of a coplanar waveguide at frequencies $f \sim 10$ GHz in both GaAs/AlGaAs and heterostructures. The oscillations were excited by electromagnetic radiation of significantly higher frequency $F \sim 100$ GHz incident on the system. The schematic diagram of the experiment is shown in the inset to Fig. 2 *a*. It can be shown that in such a scheme, the transmission of a coplanar waveguide deposited on the sample surface is determined by the system conductivity σ and geometric dimensions of the waveguide (in the formula below, the waveguide geometry determines the coefficient β):

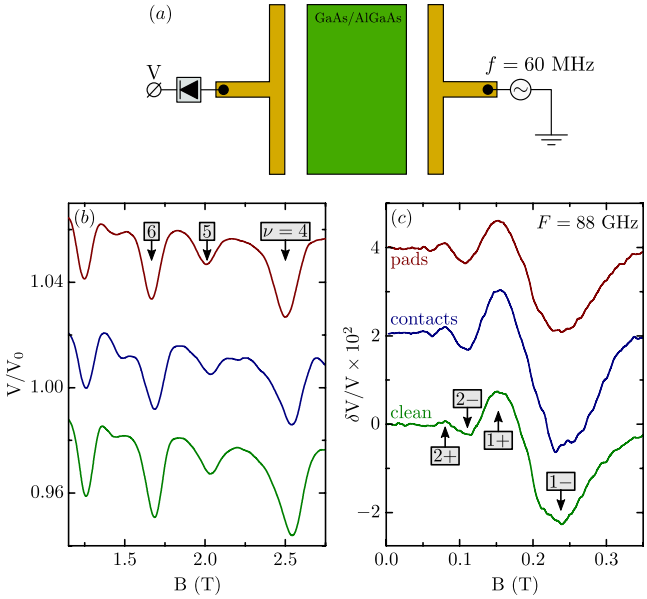

Fig. 3. (In color online) *a* — One of the schemes for contactless observation of microwave radiation-induced resistance oscillations. The sample was placed between two T-shaped antennas, one of which acted as an emitter and the second as a receiver. *b* — The detector signal at the output of the receiving antenna as a function of magnetic field in the *a* scheme shown in the panel. The radiation frequency was 60 МГц. The upper curve was obtained when a sample with a grid of metal squares on its surface was placed between the antennas, the middle curve – when a grid of ohmic contacts to the sample was formed on the sample surface, and the lower curve – in the case of a sample with a clean surface. *c* — Typical microwave radiation-induced resistance oscillations observed in such a scheme and for similar samples is determined by the high-frequency conductivity

$$P_{out} = P_{in} \exp(-\beta\sigma_{xx}). \qquad (2)$$

Here P_{in} and P_{out} are the radiation powers at the input and output of the coplanar waveguide. The value P_{out} is measured by a coaxial detector based on a Schottky diode. Fig. 2 *a* shows the dependence of the voltage at the detector output on the magnetic field. The voltage is normalized to the detector voltage V_0 in zero magnetic field. In the high field region, well-resolved Shubnikov–de Haas oscillations are observed. We marked the position of the first few filling factors. Thus, the power at the output of the coplanar waveguide indeed depends on the conductivity of the two-dimensional channel.

Fig. 2 *b* shows the correction to the detector output voltage that occurs when the excitation radiation is turned on. Note that it was amplitude-modulated, which allowed the use of lock-in amplifier technique. The positions of the first several minima and maxima are marked with arrows. When changing

the frequency, as shown in work [56], the position of oscillation extrema shifts, and the slopes of the linear magnetodispersion dependencies agree well with the results of more traditional transport experiments. Thus, it can be concluded that the presence of ohmic contacts to the two-dimensional electron system is not mandatory for observing MIRO. Moreover, it was shown that in heterojunctions GaAs/AlGaAs and ZnO/MgZnO the oscillations of high-frequency conductivity decay with increasing probe frequency f and at f>20 GHz are practically indistinguishable.

The insignificance of ohmic contacts was also demonstrated in work [57], where the possibility of observing high-frequency conductivity oscillations was shown using capacitive contacts to the system. The contacts were gold layers deposited on the structure surface. In works [58, 59] it was shown that electromagnetic radiation-induced oscillations can be observed even in the absence of any metallic layers on the sample surface. Thus, the high-frequency transport of a two-dimensional electron system formed in a quantum well GaAs/AlGaAs, was studied by measuring the power of radio-frequency radiation passing through a pair of T-shaped antennas serving as emitter and detector. The probe radiation frequency f was in the range of 10–100 MHz. The experiment geometry is schematically shown in Fig. 3 *a*.

Microwave radiation with a frequency of 60–100 GHz was delivered to the sample through an oversized waveguide. In the high field region, as shown in Fig. 3 *b*, well-resolved Shubnikov–de Haas oscillations were observed. When the excitation radiation was applied in the region of low magnetic fields, additional oscillations appeared, with amplitudes comparable to Shubnikov–de Haas oscillations in high fields. Furthermore, the introduction of ohmic contacts into the two-dimensional channel or metal layers deposited directly on the sample surface did not lead to significant changes in the amplitude of the discovered MIRO, which emphasizes the insignificance of metal layers on the sample surface for observing the effect under consideration.

3. RENORMALIZATION OF THE EFFECTIVE MASS DETERMINING THE OSCILLATION PERIOD

Let us now address the question of mass renormalization m^*, which determines the period of magnetoresistance oscillations induced by

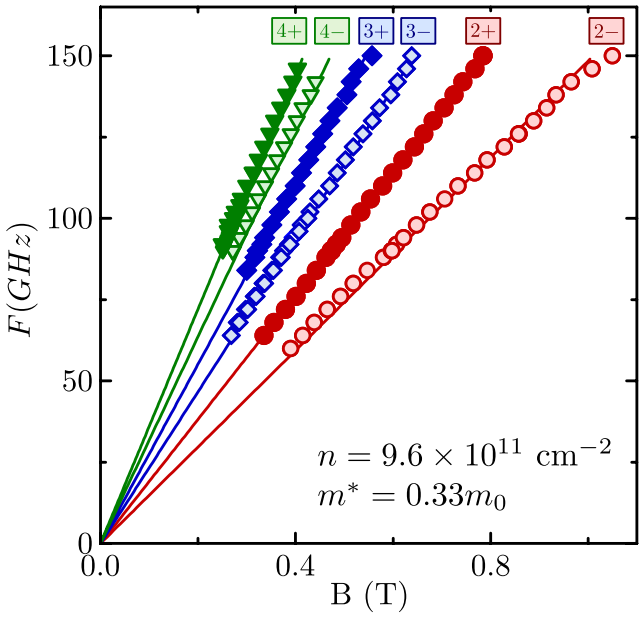

Fig. 4. (In color online) Dependencies of magnetic field position of extrema of the first several MIRO oscillations on radiation frequency. The oscillation number is indicated near each data set. Signs "+" and "–" correspond to maxima and minima. Solid lines are linear approximation of experimental data. The sample was a heterojunction ZnO/MgZnO with two-dimensional electron density $9.7 \cdot 10^{11}$ cm^{-2}

electromagnetic radiation, in more detail. Most theories describing electromagnetic radiation-induced resistance oscillations, effectively using the single-particle Drude model, assume equality between m^* and the mass extracted from the cyclotron resonance dispersion in the magnetic field/excitation frequency coordinates. However, as experimentally demonstrated in numerous works [47–50], these two masses differ significantly; moreover, it was shown that the value of m^* undergoes renormalization due to electron-electron interaction.

The value m^* is conveniently extracted the dependencies of the oscillations extrema magnetic field on the radiation frequency. This method provides the best accuracy. For example, in Fig. 1a, this frequency F was fixed at 140 GHz. When it changes, the positions of corresponding maxima and minima will shift along the magnetic field. Fig. 4 shows the dependence of their position on frequency for the same sample ZnO/MgZnO. Symbols indicate experimental data. Near each data set, the oscillation number is indicated, signs "+" or "–" denote the nature of extremum – maximum or minimum respectively. It is clearly seen that for each minimum and maximum, their position shifts linearly with

frequency, while these dependencies are well approximated by straight lines given by expression $\omega / \omega_c = k \pm 1 / 4$ with essentially a single fitting parameter m^*, in the expression $\omega_c = eB / m^*$. The resulting mass value is shown in the same figure. Note that this procedure allows obtaining mass values with very high accuracy.

In work [47], it was shown that in GaAs/AlGaAs quantum well with two-dimensional electron density $n \approx 2.7 \cdot 10^{11}$ cm^{-2} the difference between cyclotron mass and m^*, determining the period of microwave oscillations, reaches 10 %. In works [48–50] the dependence of mass m^* on two-dimensional electron density was measured in various material systems, namely in quantum wells GaAs/AlGaAs and heterojunctions ZnO/MgZnO. Note that in the case of GaAs/AlGaAs heterostructures, similar results were obtained by different groups on samples where the variation of two-dimensional density was achieved both through changing the density of donors located in the δ-doping layer, and by changing the back gate voltage.

Let's consider the case of AlGaAs quantum wells in more detail. Fig. 5 shows the dependence of the effective mass, which determines the period of resistance oscillations, on the two-dimensional density n of electrons. For comparison, a similar density dependence of the cyclotron mass is shown, as well as the Fermi-liquid mass, whose value was determined from photoluminescence spectra in zero magnetic fields and in the quantum Hall effect regime. At low densities, the mass m^*, extracted from the oscillation period increases significantly with decreasing n and becomes larger than the cyclotron mass. As shown in the figure, such behavior m^* is analogous to the behavior of the Fermi-liquid mass and has a many-body origin. Indeed, the strength of many-body interaction can be conveniently described using a dimensionless parameter r_s, which in the case of a single-valley system represents the ratio of characteristic Coulomb repulsion energy to the Fermi energy, which sets the scale of electron kinetic motion. The Coulomb interaction energy depends on the two-dimensional electron density n as $\sqrt{n}$ (inverse average distance between electrons in a two-dimensional system), while the Fermi energy is proportional to the first power of two-dimensional density n and inversely proportional to the effective mass of charge carriers. Thus, the parameter r_s is inversely proportional to $\sqrt{n}$ and linear in electron

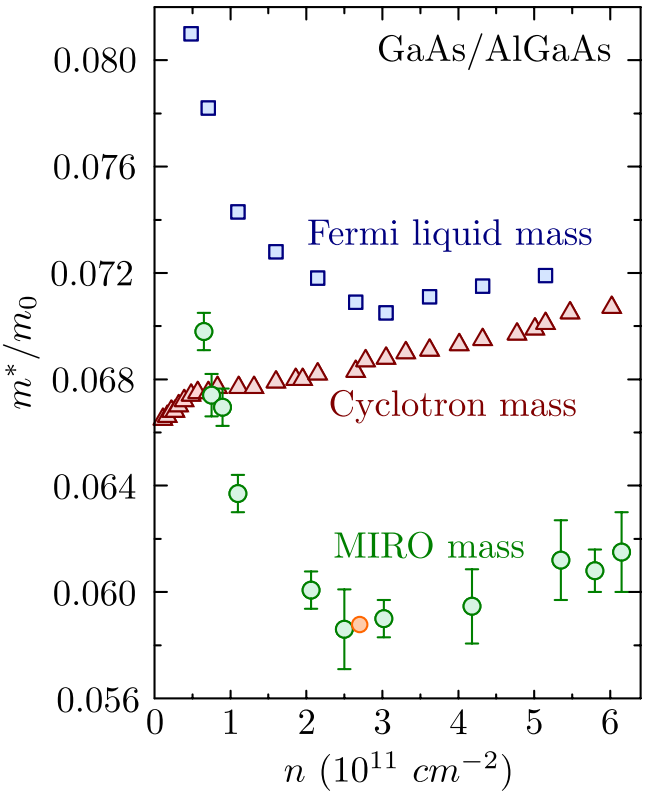

Fig. 5. (In color online) Dependence of effective mass on two-dimensional electron density in GaAs/AlGaAs heterostructures. Green circles – mass obtained from the period of radiation-induced magnetoresistance oscillations [48]. Orange circle – similar data obtained in work [47] on a sample with fixed electron density. Blue squares – Fermi liquid mass obtained from photoluminescence analysis of the electron system in magnetic field [60]. Red triangles – mass determining the cyclotron resonance dispersion [60]

mass, which means, in full agreement with the previously made conclusions, the contribution of electron-electron renormalizations should increase with decreasing two-dimensional electron density. At intermediate values of n the value of m^* reaches a minimum and grows again with increasing n. The growth in the high-density region is similar to the behavior of cyclotron mass and apparently is explained by the non-parabolicity of the electron band in GaAs. Note that the dependence of m^* on n is in many ways similar to the behavior of the effective mass that determines the activation gap, measured by the temperature dependence of the two-dimensional channel resistance near the minima of Shubnikov–de Haas oscillations in the low magnetic field region.

Additional verification of the influence of electron-electron correlations on the period of oscillations induced by electromagnetic radiation

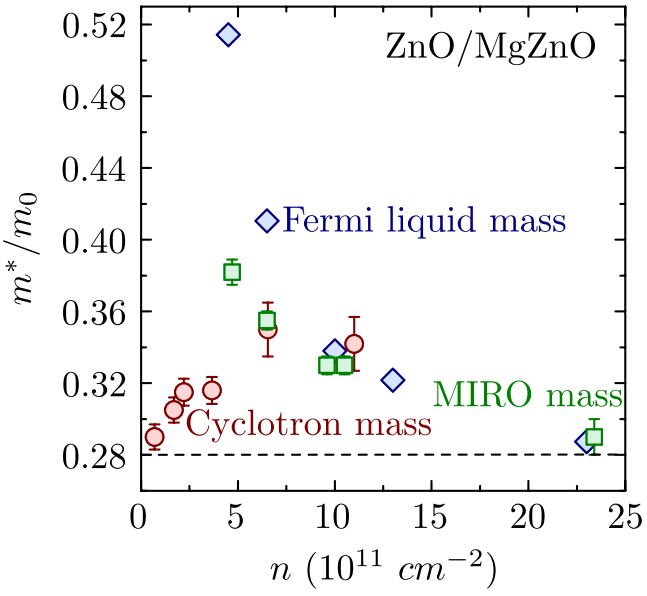

Fig. 6. (In color online) Dependence of effective mass on two-dimensional electron density in heterostructures ZnO/MgZnO. Green squares – mass obtained from the period of radiation-induced magnetoresistance oscillations [50]. Blue diamonds – Fermi liquid mass obtained from photoluminescence analysis of the electron system in magnetic field [61]. Red circles – mass determining the cyclotron resonance dispersion [62]

came from experiments in ZnO-based a material system with large charge carrier mass. For example, due to the difference in effective masses, the parameter r_s differs in heterostructures ZnO/MgZnO and GaAs quantum wells by almost an order of magnitude at the same two-dimensional density. The dependence of mass m^*, extracted from the period of microwave radiation-induced resistance oscillations, on two-dimensional density in samples ZnO/MgZnO is shown in Fig. 6. Similar to Fig. 5 cyclotron and Fermi liquid masses are also shown. All main many-body features discovered in GaAs/AlGaAs heterostructures are even stronger in ZnO/MgZnO systems.

The listed experimental results emphasize the importance of accounting for electron-electron interaction when creating theoretical models describing microwave radiation-induced magnetoresistance oscillations.

4. DIFFERENT MATERIAL SYSTEMS

GaAs/AlGaAs heterostructures remained for a long time the only material system in which microwave-induced magnetoresistance oscillations were observed, which significantly complicated the understanding of the physics of the effect under consideration. Indeed, some of the key aspects of this phenomenon significantly depend on the parameters of specific semiconductors of the heterostructure. A striking example is the renormalization of the electron effective mass, which was discussed in the previous section. Therefore, one of the most important tasks at the moment is the search for new systems in which electromagnetic radiation-induced resistance oscillations are observed.

One of the first additional semiconductor structures in which microwave-induced resistance oscillations were discovered was a two-dimensional hole system confined in a Ge quantum well with SiGe barriers [63]. The low-temperature mobility and hole density were $0.4 \cdot 10^6$ cm^2/B·c and $2.8 \cdot 10^{11}$ cm^{-2} respectively. It should be noted that in the n-channel in a similar silicon well (with similar concentrations and even higher mobilities), resistance oscillations were not observed, and the response of the two-dimensional channel resistance to microwave radiation was limited to heating effects due to magnetoplasmon excitation [64, 65].

As mentioned earlier, resistance oscillations induced by electromagnetic radiation were observed in heterostructures ZnO/MgZnO [24, 66]. Surprisingly, this phenomenon was discovered in systems with relatively low mobility $(1-5)\cdot 10^3$ cm^2/B·c, which is several orders of magnitude lower than in structures Ge/SiGe and GaAs/AlGaAs. It should also be noted that oscillations in systems ZnO/MgZnO existed only at high electron density $n > 4 \cdot 10^{11}$ cm^{-2}, while in the region of lower densities, only magnetoplasmon excitation was observed. Electromagnetic radiation-induced resistance oscillations were also detected in HgTe quantum well [67].

Similar photovoltage oscillations were observed in graphene monolayers enclosed between two relatively thick crystals of hexagonal boron nitride [68]. Moreover, such oscillations existed up to liquid nitrogen temperatures.

Resistance oscillations have also been observed in non-semiconductor structures. For instance, work [69] demonstrated that the magnetoconductivity of a two-dimensional electron channel formed on the surface of liquid helium exhibits similar oscillations under the influence of external electromagnetic radiation.

It is clearly visible that the number of systems in which electromagnetic radiation-induced resistance oscillations have been observed remains limited. Further experimental search for new structures is one of the key tasks for achieving a complete understanding of the phenomenon under consideration.

5. CIRCULAR POLARIZATION OF RADIATION

The question of sensitivity of electromagnetic radiation-induced resistance oscillations in a two-dimensional channel to the degree of circular polarization of the incident wave is crucial for establishing their nature. Theories predicting the existence of such oscillations in an infinite homogeneous electronic system explicitly assume the dependence of radiation absorption by conduction electrons on the degree of its circular polarization as $1 / [(\omega \pm \omega_c)^2 + 1 / \tau^2]$, where τ is the characteristic scattering time. The "plus" and "minus" signs here correspond to different circular polarizations of light. According to these models, the amplitude of the oscillations under consideration should demonstrate similar sensitivity. However, if sample edges, ohmic contacts, or metallic layers on the sample surface are necessary for the effect to exist, then the resistance oscillations should lose their sensitivity to radiation polarization, since the incident wave loses its circular polarization. To date, multiple attempts have not led to a definitive answer to this question, and the results of experiments by different groups yield directly opposite results.

In one of the first works devoted to this aspect of the discussed phenomenon, the dependence of oscillations on light polarization was studied in a cryostat with optical windows transparent to radiation in the sub-terahertz frequency range [40]. It was possible to achieve a very high degree of circular polarization of the wave incident on the sample. In such a scheme, it is necessary to use samples of sufficiently large size, otherwise the edges of the sample can significantly distort the radiation polarization. The degree of circular polarization of light is conveniently monitored by the amplitude of cyclotron resonance, measured by the power of radiation transmitted through the sample. The quality of the GaAs/AlGaAs-based structures used in this work was so high that it allowed observing cyclotron resonance also in longitudinal resistance. The resonance width was much smaller than the oscillation period, which made it possible to estimate its amplitude quite well. The resonance measured in this way also showed high sensitivity to the degree of circular polarization of the exciting radiation. However, the resistance oscillations proved to be insensitive to the degree of circular polarization of radiation. In work [41], similar results were obtained at higher radiation frequencies (from 0.6 THz and above). The sample was also a GaAs/AlGaAs quantum well. Note that in both works, a metal diaphragm with linear dimensions of several millimeters was located near the sample.

Several works obtained directly opposite results. For instance, experiments [70] on the surface of liquid helium showed strong sensitivity of conductivity oscillations to the degree of circular polarization of light. Also, in work [42], it was shown that in GaAs/AlGaAs heterostructures, the amplitude of resistance oscillations depends on the circular polarization of radiation. Moreover the mentioned above experiments demonstrated that when introducing a small-sized diaphragm near the sample in the optical path, the oscillations lose this sensitivity due to distortion of light polarization. The authors of the work explain the previously multiply confirmed insensitivity of oscillations to circular polarization by this circumstance.

In parallel, a series of experiments were published [71, 72], where the insensitivity of oscillation amplitude to the degree of circular polarization was again discovered. The authors of these works also demonstrated that cyclotron resonance, observed in different experimental techniques, had different dependence on light polarization: the resonance peak detected through changes in the power of radiation transmitted through the sample strongly depended on circular polarization of radiation, while the resonance measured through modification of longitudinal resistance of the system due to heating from radiation absorption was insensitive to it. Based on these experimental observations, the authors suggested that such contradictory results are consequences of radiation absorption peculiarities in the near field and are not related to the mechanism of resistance oscillations.

The above results at this stage do not allow for definitive conclusions about the sensitivity of magnetoresistance oscillation amplitude to the degree of circular polarization of the exciting

electromagnetic radiation and emphasize the relevance of further research.

6. CONCLUSION

This paper reviewed important experimental results obtained in studying the effect of microwave-induced magnetoresistance oscillations in two-dimensional electron systems. Various experimental techniques (including contactless ones) for observing this phenomenon in different material systems were discussed. Special attention was paid to the renormalization of oscillation period due to electron-electron interaction. Results of experiments analyzing the dependence of oscillation amplitude on the degree of circular polarization were considered.

FUNDING

This work was supported by the Russian Science Foundation (grant No. 19-72-30003).

REFERENCES

1. M. Zudov, R. Du, J. Simmons, and J. Reno, arXiv: cond-mat/9711149 (1997).

2. M. A. Zudov, R. R. Du, J. A. Simmons, and J. L. Reno, Phys. Rev. B 64, 201311 (2001).

3. R. G. Mani, V. Narayanamurti, K. von Klitzing et al., Phys. Rev. B 70, 155310 (2004).

4. R. G. Mani, Phys. Rev. B 72, 075327 (2005).

5. M. A. Zudov, Phys. Rev. B 69, 041304 (2004).

6. S. A. Studenikin, M. Potemski, A. Sachrajda et al., Phys. Rev. B 71, 245313 (2005)

7. A. T. Hatke, H.-S. Chiang, M. A. Zudov, L. N. Pfeiffer, and K. W. West, Phys. Rev. Lett. 101, 246811 (2008).

8. Y. Dai, R. R. Du, L. N. Pfeiffer, and K. W. West, Phys. Rev. Lett. 105, 246802 (2010).

9. A. T. Hatke, M. Khodas, M. A. Zudov, L. N. Pfeiffer, and K. W. West, Phys. Rev. B 84, 241302 (2011).

10. A. T. Hatke, M. A. Zudov, L. N. Pfeiffer, and K. W. West, Phys. Rev. Lett. 102, 066804 (2009).

11. S. A. Studenikin, A. S. Sachrajda, J. A. Gupta et al., Phys. Rev. B 76, 165321 (2007).

12. Q. Shi, S. A. Studenikin, M. A. Zudov et al., Phys. Rev. B 93, 121305 (2016).

13. A. Bogan, A. T. Hatke, S. A. Studenikin et al., Phys. Rev. B 86, 235305 (2012).

14. S. Dorozhkin, L. Pfeiffer, K. West, K. von Klitzing, and J. Smet, Nature Phys. 7, 336 (2011).

15. S. I. Dorozhkin, V. Umansky, L. N. Pfeiffer et al., Phys. Rev. Lett. 114, 176808 (2015).

16. B. Friess, V. Umansky, L. N. Pfeiffer et al., Phys. Rev. Lett. 124, 117601 (2020).

17. R. G. Mani, J. H. Smet, K. von Klitzing et al., Nature 420, 646 (2002).

18. M. A. Zudov, R. R. Du, L. N. Pfeiffer, and K. W. West, Phys. Rev. Lett. 90, 046807 (2003).

19. S. I. Dorozhkin, A. A. Kapustin, V. Umansky, K. von Klitzing, and J. H. Smet, Phys. Rev. Lett. 117, 176801 (2016).

20. A. D. Levin, G. M. Gusev, O. E. Raichev, Z. S. Momtaz, and A. K. Bakarov, Phys. Rev. B 94, 045313 (2016).

21. A. A. Bykov, JETP Lett. 87, 233 (2008).

22. S. I. Dorozhkin, I. V. Pechenezhskiy, L. N. Pfeiffer et al., Phys. Rev. Lett. 102, 036602 (2009).

23. R. G. Mani, A. N. Ramanayaka, Tianyu Ye et al., Phys. Rev. B 87, 245308 (2013).

24. D. F. Kärcherr, A. V. Shchepetilnikov, Yu. A. Nefyodov et al., Phys. Rev. B 93, 041410 (2016).

25. A. A. Bykov, J.-q. Zhang, S. Vitkalov, A. K. Kalagin, and A. K. Bakarov, Phys. Rev. B 72, 245307 (2005).

26. W. Zhang, H.-S. Chiang, M. A. Zudov, L. N. Pfeiffer, and K. W. West, Phys. Rev. B 75, 041304 (2007).

27. Q. Shi, Q. A. Ebner, and M. A. Zudov, Phys. Rev. B 90, 161301 (2014).

28. M. A. Zudov, I. A. Dmitriev, B. Friess et al., Phys. Rev. B 96, 121301 (2017).

29. A. T. Hatke, M. A. Zudov, L. N. Pfeiffer, and K. W. West, Phys. Rev. Lett. 102, 086808 (2009).

30. A. T. Hatke, M. A. Zudov, L. N. Pfeiffer, and K. W. West, Phys. Rev. B 84, 121301 (2011).

31. V. I. Ryzhii, Sov. Phys. Solid State 11, 2078 (1970).

32. V. I. Ryzhii, R. A. Suris, and B. S. Shchamkhalova, Sov. Phys. Solid State 20, 1299 (1986).

33. A. C. Durst, S. Sachdev, N. Read, and S. M. Girvin, Phys. Rev. Lett. 91, 086803 (2003).

34. M. G. Vavilov, I. A. Dmitriev, I. L. Aleiner, A. D. Mirlin, and D. G. Polyakov, Phys. Rev. B 70, 161306 (2004).

35. I. A. Dmitriev, A. D. Mirlin, and D. G. Polyakov, Phys. Rev. Lett. 91, 226802 (2003).

36. I. A. Dmitriev, M. G. Vavilov, I. L. Aleiner, A. D. Mirlin, and D. G. Polyakov, Phys. Rev. B 71, 115316 (2005).

37. I. A. Dmitriev, A. D. Mirlin, and D. G. Polyakov, Phys. Rev. B 75, 245320 (2007).

38. S. I. Dorozhkin, JETP Lett. 77, 577 (2003).

39. Y. M. Beltukov and M. I. Dyakonov, Phys. Rev. Lett. 116, 176801 (2016).

40. J. H. Smet, B. Gorshunov, C. Jiang et al., Phys. Rev. Lett. 95, 116804 (2005).

41. T. Herrmann, I. A. Dmitriev, D. A. Kozlov et al., Phys. Rev. B 94, 081301 (2016).

42. M. L. Savchenko, A. Shuvaev, I. A. Dmitriev et al., Phys. Rev. B 106, L161408 (2022).

43. A. D. Chepelianskii and D. L. Shepelyansky, Phys. Rev. B 80, 241308 (2009).

44. O. V. Zhirov, A. D. Chepelianskii, and D. L. Shepelyansky, Phys. Rev. B 88, 035410 (2013).

45. S. A. Mikhailov, Phys. Rev. B 83, 155303 (2011).

46. A. D. Chepelianskii and D. L. Shepelyansky, Phys. Rev. B 97, 125415 (2018).

47. A. T. Hatke, M. A. Zudov, J. D. Watson et al., Phys. Rev. B 87, 161307 (2013).

48. A. V. Shchepetilnikov, D. D. Frolov, Yu. A. Nefyodov, I. V. Kukushkin, and S. Schmult, Phys. Rev. B 95, 161305 (2017).

49. X. Fu, Q. A. Ebner, Q. Shi et al., Phys. Rev. B 95, 235415 (2017).

50. A. V. Shchepetilnikov, Y. A. Nefyodov, A. Dremin, and I. V. Kukushkin, JETP Lett. 107, 770 (2018).

51. C. L. Yang, M. A. Zudov, T. A. Knuuttila et al., Phys. Rev. Lett. 91, 096803 (2003).

52. P. D. Ye, L. W. Engel, D. C. Tsui et al., Appl. Phys. Lett. 79, 2193 (2001)

53. L. W. Engel, D. Shahar, I. M. C. Kurdak, and D. C. Tsui, Phys. Rev. Lett. 71, 2638 (1993).

54. V. Dziom, A. Shuvaev, A. V. Shchepetilnikov et al., Phys. Rev. B 99, 045305 (2019).

55. I. V. Andreev, V. M. Muravev, I. V. Kukushkin, S. Schmult, and W. Dietsche, Phys. Rev. B 83, 121308 (2011).

56. A. V. Shchepetilnikov, A. R. Khisameeva, Yu. A. Nefyodov, and I. V. Kukushkin, Phys. Rev. B 100, 125425 (2019).

57. A. A. Bykov, I. V. Marchishin, A. V. Goran, and D. V. Dmitriev, Appl. Phys. Lett. 97, 082107 (2010).

58. A. V. Shchepetilnikov, A. R. Khisameeva, Yu. A. Nefyodov, S. Schmult, and I. V. Kukushkin, Phys. Rev. B 102, 075445 (2020).

59. A. R. Khisameeva, A. V. Shchepetilnikov, Yu. A. Nefyodov, and I. V. Kukushkin, JETP Lett. 114, 279 (2021).

60. I. V. Kukushkin and S. Schmult, JETP Lett. 101, 693 (2015).

61. V. V. Solovyev and I. V. Kukushkin, Phys. Rev. B 96, 115131 (2017).

62. V. E. Kozlov, A. B. Van'kov, S. I. Gubarev et al., Phys. Rev. B 91, 085304 (2015).

63. M. A. Zudov, O. A. Mironov, Q. A. Ebner et al., Phys. Rev. B 89, 125401 (2014).

64. S. Sassine, Yu. Krupko, E. B. Olshanetsky et al., Sol. St. Commun. 142, 631 (2007).

65. A. R. Khisameeva, A. V. Shchepetilnikov, G. A. Nikolaev et al., JETP Lett. 118, 67 (2023).

66. D. Tabrea, I. A. Dmitriev, S. I. Dorozhkin et al., Phys. Rev. B 102, 115432 (2020).

67. M. Otteneder, I. A. Dmitriev, S. Candussio et al., Phys. Rev. B 98, 245304 (2018).

68. E. Monch, D. A. Bandurin, I. A. Dmitriev et al., Nano Lett. 20, 5943 (2020).

69. R. Yamashiro, L. V. Abdurakhimov, A. O. Badrutdinov, Y. P. Monarkha, and D. Konstantinov, Phys. Rev. Lett. 115, 256802 (2015).

70. A. A. Zadorozhko, Y. P. Monarkha, and D. Konstantinov, Phys. Rev. Lett. 120, 046802 (2018).

71. E. Mönch, P. Euringer, G.-M. Hüttner et al., Phys. Rev. B 106, L161409 (2022).

72. E. Mönch, S. Schweiss, and I. Yahniuk, arXiv:2311.05468 (2023).